Design and evaluation of surface conformance in additively manufactured spinal reconstruction implants

Richard Barina¹, Stewart McLachlin¹*

¹ Orthopaedic Biomechanics and Mechatronics Laboratory, Mechanical and Mechatronics Engineering, University of Waterloo, Waterloo, Ontario, N2L 3G1, Canada

Abstract: Spinal implant surface conformance with the underlying bone is often critical to the long-term success of spinal surgeries; however, most spinal implants have a limited ability to match the organic surface profile of the vertebral endplate. To address this challenge, this study aimed to evaluate the surface conformance of additively manufactured lumbar intervertebral cages based on bone contact area and pressure distribution. Two lateral lumbar interbody fusion (LLIF) devices with either a solid or latticed core were designed for additive manufacturing (AM). The two implants were manufactured using SLA in resin with mechanical properties similar to polyether-ether-ketone (PEEK) and in a titanium alloy (Ti64) using laser powder bed fusion. Mechanical testing occurred on three sets of polyurethane Sawbones® machined to simulate a non-uniform vertebral endplate bone. Contact area and pressure distribution were measured using the Tekscan thin film sensor under lumbar compressive waveforms applied via an AMTI VIVO system. Conventional solid implants had an average surface coverage of 19% and 16%, 1 mm of displacement motion each, and peak pressure of 4.1 to 4.8 MPa, for resin and titanium respectively. The gyroid latticed implant had 13% and 11% surface coverage, 1.46 mm and 1 mm displacement motion, and lower of peak pressure for resin and titanium respectively. These results are consistent with previous studies which found that matching the implant to the vertebral endplate stiffness reduces risks of implant subsidence. In conclusion, this study provides preliminary support for the use of AM in tailoring implant design to conform to the endplate geometry. Future work should look to evaluate surface conformance in other designs as well as consideration for testing under fatigue loading conditions.

Keywords: Latticed spinal fusion cage, contact surface, additive manufacturing, lumbar interbody fusion, compression testing.

1. Introduction

Lumbar lateral intervertebral fusion (LLIF) is a minimally invasive surgical reconstruction method to treat spinal disorders. In this procedure, the degenerated disc is removed, and an interbody device is inserted between two adjacent vertebral bodies to restore disc height and lordosis. Eventually, bone will grow over the implant providing long-term stabilization and immobilization of the joint. Spinal fusion implants are often metallic to provide the necessary structural support; however, they do not reflect the compliant and mobile nature of the spine.

Metal additive manufacturing (AM) presents an opportunity to address current shortcomings with fusion cages through the ability to produce complex structures. Several studies have been done in the field of 3D printing for spinal orthopedics such as the production of patient-specific multi-level reconstructions [1], custom trabecular bone lattices for lumbar fusions [2], and biomimicking artificial disc replacements [3]. Some alternatives to solid fusion implants have made it on the market such as the latticed ModulusTM XLIFTM or the expandable RISE-L® (Globus Medical Inc., Pennsylvania, United States). However, patient-specific cages require precise positioning to be effective [4] and there are few compliant LLIF implants.

High surface conformance of the implant with the underlying bone is often critical to the long-term success of spinal surgeries [5,6]; however, most spinal implants have a limited ability to match the organic surface profile of the vertebral endplate. To address this challenge, the goal of this study was to design and evaluate additively manufactured LLIF cages based on bone contact area and pressure distribution. Within this goal, the capabilities of AM were leveraged to design a large footprint spinal fusion implant as a solution to increase vertebral endplate contact area in challenging spinal environments.

2. Materials and methods

2.1. LLIF implant

Tohmeh et al. describe LLIF cage sizes used in disc replacement procedures in a study on the radiological and clinical evaluation of the implants [7], from which commonly used sizes for each lumbar level were extracted. Given the safe

^{*} stewart.mclachlin@uwaterloo.ca

zone for LLIF surgeries [8,9], the implant size determined to be most representative was 40 mm x 18 mm with a height of 10 mm. A mock cage was recreated in Fusion 360 (Autodesk, California, United States) as seen in Figure 1.

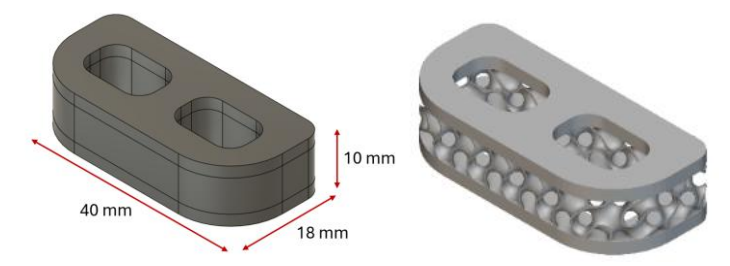


Figure 1. Left: Recreated 'Flat-solid' LLIF implant with dimensions of common size. Right: 'Flat-latticed' implant with a gyroid lattice replacing the central portion of the implant.

The implant was then modified with the idea of increasing compliance using latticing as seen on the right of Figure 1. A thin extruded feature was kept on the superior and inferior surfaces of the implant to act as the implant endplate. The lattice chosen was a triply periodic minimal surface gyroid with a thickness of 0.5 mm because of its low stiffness [10].

The implants were manufactured (Figure 2) on the Formlabs Form 3+ (Formlabs, Somerville, Massachusetts, USA) printer in Rigid 4000 resin with a layer thickness of 50 microns. This resin was chosen due to the similarity of its material properties to Polyether-ether-ketone (PEEK), a common biomaterial [4]. In addition, a set of titanium alloy (Ti6Al4V/Ti64) implants were printed using laser powder bed fusion (LPBF) on the Renishaw AM400 (Wotton-under-Edge, England) system in partnership with the MSAM laboratory at the University of Waterloo using previously developed process parameters. No post-processing was applied.



Figure 2. Left: Resin printed implants (flat-solid and flat-latticed). Right: Ti64 printed implants (flat-solid and flat-latticed).

2.2. Testing methods

Testing was conducted on the AMTI VIVO (AMTI, Watertown, Massachusetts, USA) six degree of freedom (6DOF) joint motion simulator fitted with custom fixturing on three Sawbone specimens (n=3). The fixtures were designed to simulate a challenging vertebral endplate geometry in a repeatable fashion, similar to the setup used by Kusins et al. [11]. The experimental setup (Figure 3) consists of an LLIF implant placed on a machined block of standardized polyurethane Sawbones (20 pounds per cubic foot; Pacific Research Laboratories Inc., Vashon, Washington, USA) selected to simulate vertebral endplate bone [5].

A Tekscan thin-film pressure sensor (Sensor 5051; Tekscan, Norwood, Massachusetts, USA) was used to measure the contact area and pressure distribution of the experiment. The sensor was placed between the Sawbone sample and the implant as this was the critical measurement surface. The Tekscan sensor was calibrated once at the beginning of the testing after initial preconditioning.

The applied waveform was a sinusoidal 500 N compressive load with no movement about all other degrees of freedom simulating a vertical compression test rig. It was applied for 5 cycles at a frequency of 0.05 Hz. Load and displacement data was collected using the load cell on the AMTI VIVO which was reset to it's reference pose before each test.

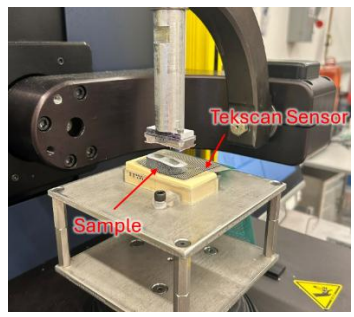


Figure 3. Test configuration. The Tekscan sensor and sample are indicated in red and lie on top of the Sawbone specimen.

2.3. Contact area analysis

The implants were randomly selected for testing using a blind pick method for each test. The area data from the Tekscan was manually aligned to the load cell data from the VIVO. The data for each implant type was averaged over three of the five cycles then between the three Sawbones specimens. The contact footprint (percent area) was calculated as the measured Tekscan area over the implants inferior endplate surface area computed from the CAD model.

The pressure on the implant was approximated using the force data from the load cell on the VIVO because the Tekscan sensor cells saturated at the calibrated sensitivity. This was achieved by taking the magnitude of the three components of force over the measured area after aligning the data. It was assumed that moments were not significant and did not affect the pressure.

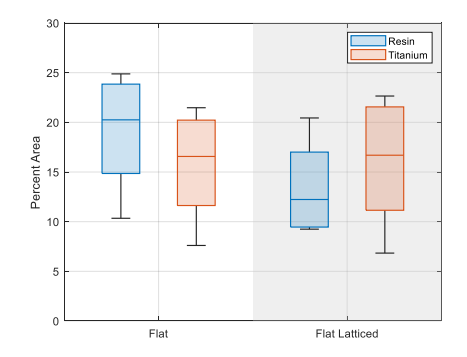
3. Results and discussion

Overall, the four implants were tested three times each. The latticed resin implant failed in all three tests at an average of -149 N and was replaced each time. Failure occurred at the lateral edge of the implant where a pressure concentration was noted from the challenging endplate geometry.

3.1. Contact area

The average percent area for the flat samples up to 500 N was 19.1 in resin and 15.7 in titanium. In the latticed samples, the average percent area found was 13.3 in resin and 16.1 in titanium; however, the resin failed at 149 N of compression while the titanium reached 500 N. Except in the case of the failed resin lattice, the range of area experienced during the waveform is similar between implants as shown in Figure 4.

Comparing the all the implants up to 149 N, the average contact footprint for the flat sample was 14.7 in resin and 11.0 in titanium. The average contact footprint in the latticed sample was found to be 13.3 in resin and 10.7 in titanium. These values are lower compared to the full waveform. In addition to a higher average, the range of contact area experienced by the resin implants is larger than that of the titanium, indicating more deformation during the waveform. Furthermore, the latticed implants have a larger range than the solid implants.



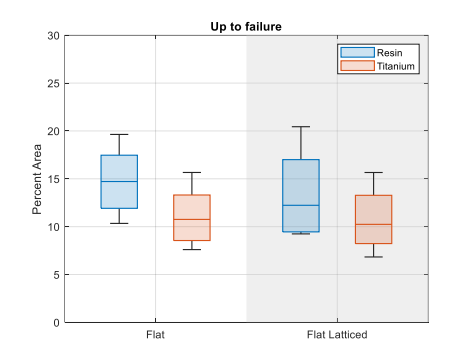


Figure 4. Percent of the bottom implant surface area used during the compression testing. Left: Full waveform up to 500N. Right: Contact footprint only considering loads up to -150N.

3.2. Displacements

The maximum end effector displacement for the solid cages was approximately 1 mm in both resin and titanium (Table 1). The latticed resin cage had a displacement of 1.46 mm while the titanium cage had a displacement of 1 mm similarly to the solid cages. These results highlight that the mechanical behavior of the latticed feature varies with material, demonstrating the potential for material-specific tuning of implant compliance.

Table 1. Vertical displacement of each sample.

Type	Resin [mm]	Titanium [mm]
Flat	1.07 ±0.37	1.05 ± 0.36
Flat latticed	1.46 ± 0.31	1.06 ± 0.36

3.3. Contact pressure

Figure 5 shows that the maximum pressure of the solid cages was 4.11 MPa and 4.80 MPa in resin and titanium respectively. The latticed resin sample reached a maximum pressure of 1.53 MPa but it can be seen to start deforming plastically after 1.2 MPa. The latticed titanium was found to have a lower maximum pressure (4.52 MPa) than its solid counterpart but more pressure than the solid resin.

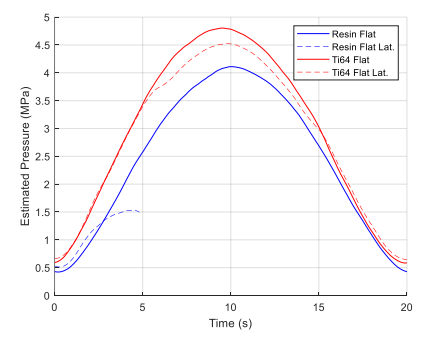


Figure 5. Estimated pressure of the cage samples. The resin cages have an overall lower pressure than the titanium cages.

Fernandes et al. [4] performed a biomechanical comparison of the subsidence of patient specific versus commercially available posterior LIF (PLIF) implants (n=5). The patient specific cages were designed using reconstructed vertebral models from CT scans of cadaveric specimens. Results showed that patient specific cages had an implant-bone interface up to 1.6x stiffer and required a 64 % increase in the force to subside over their commercial counterparts. The conclusion was that closely matching the surface of the vertebral body reduces the risk of complications postoperatively; however, patient specific implants take expert preoperative planning and precise placement, both of which are difficult to achieve. As this study was performed on PLIF implants, it does not necessarily translate to larger implants like LLIF implants, which the current work expanded upon using similar methods.

4. Conclusion

The present study aimed to evaluate the contact footprint and pressure distribution of additively manufactured LLIF cages. The results show that the PEEK-like resin implant reduces contact pressure and accommodates greater deformation compared to the titanium one. Incorporating a lattice further increases the contact area and enhances compliance, indicating that material selection combined with lattice architecture can be strategically used to optimize implant performance. Future work should investigate recent advancements in AM of metamaterials and their application towards compliant LLIF implants and testing under fatigue loading conditions.

5. Acknowledgments

We would like to acknowledge the support of Claire Thompson for mechanical testing assistance.

6. References

- [1] Kang J, Dong E, Li X, Guo Z, Shi L, Li D, et al. Topological design and biomechanical evaluation for 3D printed multi-segment artificial vertebral implants. Materials Science and Engineering: C 2021;127:112250. https://doi.org/10.1016/j.msec.2021.112250.
- [2] Tartara F, Bongetta D, Pilloni G, Colombo EV, Giombelli E. Custom-made trabecular titanium implants for the treatment of lumbar degenerative discopathy via ALIF/XLIF techniques: rationale for use and preliminary results. Eur Spine J 2020;29:314–20. https://doi.org/10.1007/s00586-019-06191-y.
- [3] Yu Z, Voumard B, Shea K, Stanković T. Exploration of the influence of different biomimetic designs of 3D printed multi-material artificial spinal disc on the natural mechanics restoration. Materials & Design 2021;210:110046. https://doi.org/10.1016/j.matdes.2021.110046.
- [4] Fernandes RJR, Gee A, Kanawati AJ, Siddiqi F, Rasoulinejad P, Zdero R, et al. Evaluation of the contact surface between vertebral endplate and 3D printed patient-specific cage vs commercial cage. Sci Rep 2022;12:12505. https://doi.org/10.1038/s41598-022-16895-9.
- [5] Tatsumi R, Lee Y-P, Khajavi K, Taylor W, Chen F, Bae H. In vitro comparison of endplate preparation between four mini-open interbody fusion approaches. Eur Spine J 2015;24:372–7. https://doi.org/10.1007/s00586-014-3708-x.
- [6] Chien K-T, Feng H-W, Chang T-K, Liu Y-C, Chen L-P, Huang Y-C, et al. Optimizing Disc and Cartilage Endplate Preparation in Full-Endoscopic Lumbar Interbody Fusion: An In-Depth Exploration of Surgical Instruments with a Technique Note and Narrative Review. World Neurosurgery 2024;189:228–47. https://doi.org/10.1016/j.wneu.2024.06.074.
- [7] Tohmeh AG, Khorsand D, Watson B, Zielinski X. Radiographical and Clinical Evaluation of Extreme Lateral Interbody Fusion: Effects of Cage Size and Instrumentation Type With a Minimum of 1-Year Follow-up. Spine 2014;39:E1582. https://doi.org/10.1097/BRS.0000000000000645.
- [8] Guérin P, Obeid I, Gille O, Bourghli A, Luc S, Pointillart V, et al. Safe working zones using the minimally invasive lateral retroperitoneal transpsoas approach: a morphometric study. Surg Radiol Anat 2011;33:665–71. https://doi.org/10.1007/s00276-011-0798-6.
- [9] Quack V, Eschweiler J, Prechtel C, Migliorini F, Betsch M, Maffulli N, et al. L4/5 accessibility for extreme lateral interbody fusion (XLIF): a radiological study. Journal of Orthopaedic Surgery and Research 2022;17:483. https://doi.org/10.1186/s13018-022-03320-0.
- [10] Gross V, Zankovic S, Rolauffs B, Velten D, Schmal H, Seidenstuecker M. On the suitability of additively manufactured gyroid structures and their potential use as intervertebral disk replacement a feasibility study. Front Bioeng Biotechnol 2024;12:1432587. https://doi.org/10.3389/fbioe.2024.1432587.
- [11] Kusins J, Uyekawa S, Singh G, Peng Y, McQuarrie C, Holman P, et al. A Lateral Expandable Cage with Independently Adjustable Anterior and Posterior Heights Can Improve the Pressure Distribution at the Cage-Endplate Interface: A Biomechanics Study. World Neurosurgery 2024;181:e722–31. https://doi.org/10.1016/j.wneu.2023.10.118.